A Reynolds uniform numerical method for Prandtl's boundary layer problem for flow past a three dimensional yawed wedge

J.S. Butler
Department of Mathematics, Trinity College, Dublin, Ireland.
J.J.H Miller
Department of Mathematics, Trinity College, Dublin, Ireland & Department of Computational Science, National University of Singapore, Singapore.
G.I. Shishkin
Institute for Mathematics and Mechanics, Russian Academy of Sciences, Ekaterinburg, Russia

Abstract We consider Prandtl's boundary layer problem for incompressible laminar flow past a three dimensional yawed wedge. When the Reynolds number is large the solution of this problem has a parabolic boundary layer. We construct a direct numerical method for computing approximations to the solution of this problem using a compound piecewise-uniform mesh appropriately fitted to the parabolic boundary layer. Using this numerical method we approximate the self–similar solution of Prandtl's problem in a finite rectangle excluding the leading edge of the wedge, which is the source of an additional singularity caused by incompatibility of the problem data. By means of extensive numerical experiments, for ranges of values of the Reynolds number, wedge angle and number of mesh points, we verify that the constructed numerical method is Reynolds and angle uniform, in the sense that the computed errors and orders of convergence for the velocity components and their derivatives in the discrete maximum norm are Reynolds and angle uniform. We use a special numerical method related to the Blasius technique to compute a semi–analytic reference solution with required accuracy for use in the error analysis.

Keywords: Yawed wedge flow, Prandtl boundary layer, numerical method, Reynolds- and angle- uniform.

1 Introduction

Incompressible laminar flow past a three dimensional semi-infinite yawed wedge W in the domain D = $\mathbf{R}^3\backslash$W is governed by the Navier-Stokes equations. Using Prandtl's approach the vertical momentum equation is omitted and the horizontal momentum equation is simplified, see [2].

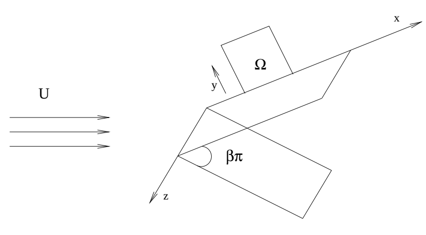

Figure 1: Flow past a wedge

The new momentum equation is parabolic and singularly perturbed, which means that the highest order derivative is multiplied by a small singular perturbation parameter. In this case the parameter is the reciprocal of the Reynolds number. For convenience we use the notation $\varepsilon = \frac{1}{Re}$. It is well known that for flow problems with large Reynolds numbers a boundary layer arises on the surface of the wedge. Also, when classical numerical methods are applied to these problems large errors occur, especially in approximations of the derivatives, which grow unboundedly as the Reynolds number increases. For this reason robust layer-resolving numerical methods, in which the error is independent of the singular perturbation parameter, are required. We want to solve the Prandtl problem in a region including the parabolic boundary layer. Since the solution of the problem has another singularity at the leading edge of the wedge, we take as the computational domain the finite rectangle $\Omega = (.1, 1.1) \times (0, 1)$ on the upper side of the wedge in the x, y plane, which is sufficiently far from the leading edge (see fig. 2) that the leading edge singularity does not cause problems for the numerical method. We denote the boundary of Ω by $\Gamma = \Gamma_L \bigcup \Gamma_T \bigcup \Gamma_B \bigcup \Gamma_R$ where Γ_L, Γ_T, Γ_B and Γ_R denote, respectively the left-hand, top, bottom and right-hand edges of Ω. The Prandtl boundary layer problem in Ω is:

$$(P_\varepsilon)\begin{cases} \text{Find } \mathbf{u}_\varepsilon = (u_\varepsilon, v_\varepsilon, w_\varepsilon) \text{ such that for all } (x, y, z) \in \Omega \\ \mathbf{u}_\varepsilon \text{ satisfies the differential equations} \\ \\ -\frac{1}{Re}\frac{\partial^2 u_\varepsilon}{\partial^2 y} + u_\varepsilon \frac{\partial v_\varepsilon}{\partial x} + v_\varepsilon \frac{\partial u_\varepsilon}{\partial y} = U\frac{dU}{dx} \\ \\ -\frac{1}{Re}\frac{\partial^2 w_\varepsilon}{\partial^2 y} + u_\varepsilon \frac{\partial w_\varepsilon}{\partial x} + v_\varepsilon \frac{\partial w_\varepsilon}{\partial y} = 0 \\ \\ \frac{\partial u_\varepsilon}{\partial x} + \frac{\partial v_\varepsilon}{\partial y} = 0 \\ \\ \text{with boundary conditions} \\ u_\varepsilon = 0, \quad w_\varepsilon = 0 \text{ and } v_\varepsilon = 0 \text{ on } \Gamma_B \\ \mathbf{u}_\varepsilon = \mathbf{u}_P \quad \Gamma_L \bigcup \Gamma_T \end{cases}$$

where $U(x) = x^m$, $m = \frac{\beta}{2-\beta}$ and $\beta\pi$ is the angle of the wedge in radians.
Our goal is to construct an (Re, β)–uniform numerical method for solving (P_ε), in the sense that the method has error bounds, for the solution and its derivatives, independent of Re and β, for all $Re \in [1, \infty)$ and all $\beta \in [0, 1]$.

2 Blasius similarity solution

Using the similarity transformation (see, for example, Reference [4])

$$\eta = y\sqrt{\frac{(m + 1.0)Re}{2xU}}$$

the velocity components of the Blasius' solution $\mathbf{u}_B$ of (P_ε) are given in terms of f and g by

$$u_B(x, y) = Uf'(\eta), \quad v_B(x, y) = -\sqrt{\frac{(m+1)\varepsilon U}{2x}}(f + \frac{m-1}{m+1}\eta f'(\eta)), \quad w_B(x, y) = g(\eta)$$

and their scaled derivatives by similar expressions, for example

$$\frac{\partial u_B}{\partial y} = U\sqrt{\frac{(m+1.0)Re}{2xU}}f^{''}(\eta)$$

where f and g are the solutions of the coupled non–linear problem

$$(P_B)\begin{cases} \text{Find } f \in C^3([0,\infty)) \text{ such that for all } \eta \in [0,\infty) \\ \\ f^{'''}(\eta) + f(\eta)f^{''}(\eta) + \beta(1 - f^{'2}(\eta)) = 0 \\ \\ g^{''}(\eta) + f(\eta)g^{'}(\eta) = 0 \\ \\ f(0) = g(0) = 0, \quad f^{'}(0) = 0, \quad \lim_{\eta\to\infty} f^{'}(\eta) = 1 \quad \lim_{\eta\to\infty} g(\eta) = 1. \end{cases}$$

To find the components u_B, v_B and w_B of $\mathbf{u_B}$, and their derivatives, on the finite domain Ω for all $Re \in [1,\infty)$, we need to solve (P_B) numerically for f and g and their derivatives on the semi-infinite domain $[0,\infty)$. Then we apply post-processing to determine numerical approximations to $\mathbf{u}_\varepsilon$. An analogous process is described in detail in [5] for flow past a two dimensional wedge.
Here, we make use of the Blasius similarity solution of Prandtl's problem in two ways. First, we use it to provide the required artificial boundary conditions on the boundary of Ω in the direct numerical method for Prandtl's problem discussed in the next section. Secondly, we use it as a reference solution for the unknown exact solution in the expression for the error. Since the Blasius solution is known to converge (Re,β)–uniformly to the solution of Prandtl's problem, we can compute (Re,β)–uniform error bounds. For this purpose we use the Blasius solution for (P_B) when N=8192, namely $\mathbf{U}_B^{8192}$, which provides the required accuracy for the velocity components U_B^{8192}, V_B^{8192}, W_B^{8192}, their derivatives $D_xV_B^{8192}$, $D_yV_B^{8192}$, $D_xW_B^{8192}$ and their scaled derivatives $\sqrt{\varepsilon}D_yU_B^{8192}$, $\sqrt{\varepsilon}D_yW_B^{8192}$.

3 Direct Numerical method for Prandtl's Problem

The aim of this section is to construct a direct numerical method to solve the Prandtl problem (P_ε) for all $Re \in [1,\infty)$ and all $\beta \in [0,1]$. We require a piecewise uniform fitted mesh $\Omega_\varepsilon^{\mathbf{N}}$ in the rectangle Ω, where $\mathbf{N}$=(N_x, N_y). We define the mesh as the tensor product $\Omega_\varepsilon^{\mathbf{N}} = \Omega_u^{N_x} \times \Omega_\varepsilon^{N_y}$, where the one–dimensional mesh in the x direction is the uniform mesh $\Omega_u^{N_x} = \{x_i : x_i = 0.1 + iN_x^{-1}, 0 \le i \le N_x\}$ and the mesh in the y-direction is the piecewise–uniform fitted mesh

$$\Omega_\varepsilon^{N_y} = \{y_j : y_j = \sigma j\frac{2}{N_y}, 0 \le j \le \frac{N_y}{2}; y_j = \sigma + (1-\sigma)(j - \frac{N_y}{2})\frac{2}{N_y}, \frac{N_y}{2} \le j \le N_y\}.$$

It is important to note that the transition point σ is chosen so that there is a fine mesh in the boundary layer whenever it is required. The appropriate choice in this case is

$$\sigma = \min\{\frac{1}{2}, \sqrt{\varepsilon}lnN_y\}.$$

The factor $\sqrt{\varepsilon}$ may be motivated from *a priori* estimates of the derivatives of the solution $\mathbf{u}_\varepsilon$ or from asymptotic analysis. For simplicity we take $N_x = N_y = N$.
The problem (P_ε) is discretized by the following non-linear upwind finite difference method on the piecewise uniform fitted mesh $\Omega_\varepsilon^{\mathbf{N}}$

$$(P_\varepsilon^N)\begin{cases} \text{Find } \mathbf{U}_\varepsilon = (U_\varepsilon, V_\varepsilon, W_\varepsilon) \text{ such that for all mesh points } (x_i, y_j) \in \Omega_\varepsilon^{\mathbf{N}} \\ \mathbf{U}_\varepsilon \text{ satisfies the finite mesh difference equations} \\ \\ -\varepsilon\delta_y^2 U_\varepsilon(x_i, y_j) + U_\varepsilon D_x^- U_\varepsilon(x_i, y_j) + V_\varepsilon D_y^u U_\varepsilon(x_i, y_j) = U\frac{dU}{dx} \\ \\ -\varepsilon\delta_y^2 W_\varepsilon(x_i, y_j) + U_\varepsilon D_x^- W_\varepsilon(x_i, y_j) + V_\varepsilon D_y^u W_\varepsilon(x_i, y_j) = 0 \\ \\ D_x^- U_\varepsilon(x_i, y_j) D_y^- V_\varepsilon(x_i, y_j) = 0 \\ \\ \text{with boundary conditions} \\ U_\varepsilon = 0, \quad W_\varepsilon = 0 \text{ and } V_\varepsilon = 0 \text{ on } \Gamma_B \\ U_\varepsilon = U_B \text{ and } W_\varepsilon = W_B \ \ \Gamma_L \bigcup \Gamma_T \end{cases}$$

where D_x^-, D_x^+ and D_y^-, D_y^+ are the standard first–order backward, respectively forward, finite difference operators in the x and y directions and, for any continuous function V_ε on the domain $\Omega_\varepsilon^{\mathbf{N}}$, the upwind finite difference operator D_y^u is defined by

$$V_\varepsilon(x_i, y_j) D_y^u U_\varepsilon(x_i, y_j) = \begin{cases} V_\varepsilon(x_i, y_j) D_y^- U_\varepsilon(x_i, y_j) & \text{if } V_\varepsilon(x_i, y_j) \geq 0 \\ V_\varepsilon(x_i, y_j) D_y^+ U_\varepsilon(x_i, y_j) & \text{if } V_\varepsilon(x_i, y_j) < 0 \end{cases}$$

and δ_y^2 is the standard second order centered finite difference operator in the y direction. Changes between forward and backward differences are required because at angles $\beta > 0.1$, V_ε is initially negative and then becomes positive. Note that, without these changes, the tridiagonal system is no longer diagonally dominant and the continuation algorithm fails to converge.
Since $(P_\varepsilon^{\mathbf{N}})$ is a non–linear finite difference method an iterative method is required for its solution. This is obtained by replacing the system of non–linear equations by the following sequence of

systems of linear equations

$$
(A_\varepsilon^{\mathbf{N}})\left\{
\begin{array}{l}
\text{With the boundary condition } \mathbf{U}_\varepsilon^{\mathbf{M}} = \mathbf{U}_{\mathrm{B}}^{\mathbf{8192}} \text{ on } \Gamma_{\mathrm{L}}, \text{for each } i, 1 \le i \le N,\\
\text{use the initial guess } \mathbf{U}_\varepsilon^0|_{X_i} = \mathbf{U}_\varepsilon^{M_{i-1}}|_{X_{i-1}} \text{and for } \ m = 1, \ldots, M_i \ \text{ solve the following}\\
\text{two point boundary value problem for } U_\varepsilon^m(x_i, y_j)\\
\\
-\varepsilon\delta_y^2 U_\varepsilon^m(x_i, y_j) + U_\varepsilon^{m-1} D_x^- U_\varepsilon^m(x_i, y_j) + V_\varepsilon^{m-1} D_y^u U_\varepsilon^m(x_i, y_j) = U\frac{dU}{dx} \quad 1 \le j \le N-1\\
\\
\text{with the boundary conditions } U_\varepsilon^m = U_{\mathrm{B}} \text{ on } \Gamma_{\mathrm{B}} \cup \Gamma_{\mathrm{T}}, \text{and the initial guess for } V_\varepsilon^0|_{X_1} = 0.\\
\text{Also solve the initial value problem for } V_\varepsilon^m(x_i, y_j)\\
\\
D_x^- U_\varepsilon^m(x_i, y_j) + D_y^- V_\varepsilon^m(x_i, y_j) = 0\\
\\
\text{with initial condition } V_\varepsilon^m = 0 \text{ on } \Gamma_{\mathrm{B}}.\\
\text{Continue to iterate between the equations for } \mathbf{U}_\varepsilon^m \text{ until } m = M_i, \text{where } M_i \text{ is such that}\\
\max(|U_\varepsilon^{M_i} - U_\varepsilon^{M_i-1}|_{\overline{X}_i}, \frac{1}{V^*}|V_\varepsilon^{M_i} - V_\varepsilon^{M_i-1}|_{\overline{X}_i}) \le tol.\\
\text{Finally, solve the two point boundary value problem for } W_\varepsilon(x_i, y_j)\\
\\
-\varepsilon\delta_y^2 W_\varepsilon(x_i, y_j) + U_\varepsilon^{M_i} D_x^- W_\varepsilon(x_i, y_j) + V_\varepsilon^{M_i} D_y^u W_\varepsilon(x_i, y_j) = 0, \quad 1 \le j \le N-1\\
\\
\text{with the boundary conditions } W_\varepsilon = W_{\mathrm{B}} \text{ on } \Gamma_{\mathrm{B}} \cup \Gamma_{\mathrm{T}}.
\end{array}\right.
$$

For notational simplicity, we suppress explicit mention of the iteration superscript M_i, and henceforth we write simply $\mathbf{U}_\varepsilon$ for the solution generated by $(A_\varepsilon^{\mathbf{N}})$. We take $tol = 10^{-6}$ in the computations. We note that there are no known theoretical results concerning the convergence of the solutions $\mathbf{U}_\varepsilon$ of $(P_\varepsilon^{\mathbf{N}})$ to the solution $\mathbf{u}_\varepsilon$ of (P_ε) and no theoretical estimate for the pointwise error $(\mathbf{U}_\varepsilon - \mathbf{u}_\varepsilon)(x_i, y_j)$. It is for this reason that in the error analysis of the next section, we are forced to use controllable experimental techniques, which are adapted to the problem under consideration and are of crucial value to our understanding of these computational problems.

4 Error Analysis

In this section, we compute Reynolds–uniform maximum pointwise errors in the approximations generated by the direct numerical method described in the previous section. For the sake of brevity, we discuss the approximate errors and rates of convergence in the scaled velocity components and their discrete first order x- and y- derivatives for only one value of the wedge angle, namely $\beta = 0.7$.These show that the method is Re-uniform for $\beta = 0.7$. Further computations, not reported here, show that it is (Re, β)-uniform for all $Re \in [1, \infty)$, $\beta \in [0, 1]$. The appropriate scaling factor for the vertical velocity is $V^* = \max_{\Omega_\varepsilon^N} V_B^{8192}$.
We compare the approximations generated by the direct numerical method (A_ε^N) of the previous section with the corresponding values of U_B^{8192}. We use the following definitions for the errors

$$E_\varepsilon^{\mathbf{N}}(U_\varepsilon) = ||U_\varepsilon - \overline{U_B}^{8192}||_{\overline{\Omega}_\varepsilon^N}, \quad E_\varepsilon^{\mathbf{N}}(\tfrac{1}{V^*}V_\varepsilon) = \tfrac{1}{V^*}||V_\varepsilon - \overline{V_B}^{8192}||_{\overline{\Omega}_\varepsilon^N}$$

$$E_\varepsilon^{\mathbf{N}}(W_\varepsilon) = ||W_\varepsilon - \overline{W_B}^{8192}||_{\overline{\Omega}_\varepsilon^N}.$$

$\varepsilon \backslash N$	32	64	128	256	512
2^{-0}	5.16e-04	2.90e-04	1.56e-04	8.50e-05	4.65e-05
2^{-2}	3.19e-03	1.69e-03	8.73e-04	4.43e-04	2.22e-04
2^{-4}	6.84e-03	3.52e-03	1.78e-03	8.94e-04	4.44e-04
2^{-6}	8.97e-03	4.68e-03	2.35e-03	1.17e-03	5.81e-04
2^{-8}	9.33e-03	4.90e-03	2.54e-03	1.31e-03	6.66e-04
.	.	.	.	.	.
2^{-20}	9.22e-03	4.90e-03	2.54e-03	1.31e-03	6.66e-04

Table 1: Computed maximum pointwise error $E_\varepsilon^{\mathbf{N}}(U_\varepsilon)$ where U_ε is generated by (A_ε^N) for various values of ε, N and $\beta = 0.7$

$\varepsilon \backslash N$	32	64	128	256	512
2^{-0}	8.72e-02	4.54e-02	2.41e-02	1.29e-02	7.10e-03
2^{-2}	5.13e-02	2.65e-02	1.36e-02	7.02e-03	3.71e-03
2^{-4}	3.47e-02	1.77e-02	8.99e-03	4.60e-03	2.38e-03
2^{-6}	2.82e-02	1.51e-02	7.69e-03	3.91e-03	2.00e-03
2^{-8}	2.17e-02	1.14e-02	6.04e-03	3.19e-03	1.68e-03
2^{-10}	1.88e-02	9.64e-03	5.00e-03	2.58e-03	1.34e-03
2^{-12}	1.73e-02	8.81e-03	4.50e-03	2.30e-03	1.17e-03
2^{-14}	1.67e-02	8.40e-03	4.26e-03	2.16e-03	1.09e-03
2^{-16}	1.63e-02	8.19e-03	4.14e-03	2.09e-03	1.05e-03
2^{-18}	1.61e-02	8.09e-03	4.08e-03	2.05e-03	1.03e-03
2^{-20}	1.61e-02	8.04e-03	4.05e-03	2.03e-03	1.02e-03

Table 2: Computed maximum pointwise error $E_\varepsilon^{\mathbf{N}}(\frac{1}{V^*}V_\varepsilon)$ where V_ε is generated by (A_ε^N) for various values of ε, N and $\beta = 0.7$

$\varepsilon \backslash N$	32	64	128	256	512
2^{-0}	3.00e-03	1.65e-03	8.91e-04	4.79e-04	2.62e-04
2^{-2}	8.07e-03	4.28e-03	2.26e-03	1.21e-03	6.78e-04
2^{-4}	8.33e-03	4.44e-03	2.34e-03	1.25e-03	7.01e-04
2^{-6}	9.82e-03	5.72e-03	3.04e-03	1.61e-03	8.76e-04
2^{-8}	9.82e-03	5.82e-03	3.34e-03	1.90e-03	1.09e-03
.	.	.	.	.	.
2^{-20}	9.82e-03	5.82e-03	3.34e-03	1.90e-03	1.09e-03

Table 3: Computed maximum pointwise error $E_\varepsilon^{\mathbf{N}}(W_\varepsilon)$ where W_ε is generated by (A_ε^N) for various values of ε, N and $\beta = 0.7$

The numerical results in Tables 1, 2 and 3, respectively, indicate that the method is Re-uniform for the scaled velocity components U_ε, $\frac{1}{V^*}V_\varepsilon$ and W_ε.

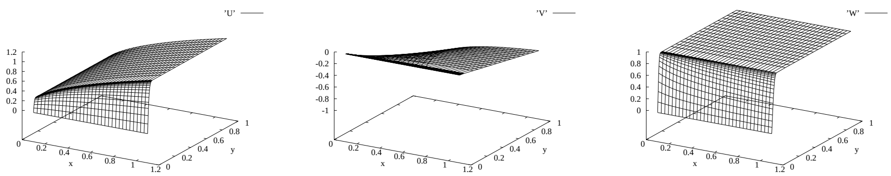

Figure 2: Graphs of U_ε^N, $\frac{1}{V^*}V_\varepsilon$ and W_ε for $\varepsilon = 2^{-8}$, N=32 and $\beta = 0.7$.

In Figure 2 we see that the computed scaled velocity components have no non-physical oscillations. The boundary layer on the surface of the wedge is apparent for both velocity components U_ε and W_ε.
We define the computed local order of convergence $p^N_{\varepsilon,comp}$ for the velocity component U_ε^N and the Re–uniform order p^N_{comp} by

$$p^N_{\varepsilon,comp} = log_2 \frac{||U_\varepsilon^N - U_B^{8192}||_{\Omega_\varepsilon^N}}{||U_\varepsilon^{2N} - U_B^{8192}||_{\Omega_\varepsilon^{2N}}} \quad p^N_{comp} = log_2 \frac{\max_\varepsilon ||U_\varepsilon^N - U_B^{8192}||_{\Omega_\varepsilon^N}}{\max_\varepsilon ||U_\varepsilon^{2N} - U_B^{8192}||_{\Omega_\varepsilon^{2N}}}$$

with analogous expressions for the velocity components V_ε^N and W_ε^N. In Tables 4-6 we give the numerical results for these computed Re–uniform orders of convergence. We see that for all N the order of convergence for the approximations to the scaled velocity components in each case is at least 0.76. This indicates that for the velocity components the method is Re-uniform for $\beta = 0.7$.

$\varepsilon \backslash N$	32	64	128	256
2^{-0}	0.83	0.89	0.88	0.87
2^{-2}	0.91	0.96	0.98	0.99
2^{-4}	0.96	0.98	1.00	1.01
2^{-6}	0.94	0.99	1.00	1.01
2^{-8}	0.93	0.95	0.96	0.97
2^{-10}	0.92	0.95	0.96	0.97
.	.	.	.	.
2^{-20}	0.91	0.95	0.96	0.97
p^N_{comp}	0.92	0.95	0.96	0.97

Table 4: Computed orders of convergence $p^N_{\varepsilon,comp}$, p^N_{comp} for $U_\varepsilon - \overline{U_B^{8192}}$ where U_ε is generated by (A_ε^N) for various values of ε, N and $\beta = 0.7$

$\varepsilon \backslash N$	32	64	128	256
2^{-0}	0.94	0.92	0.90	0.87
2^{-2}	0.96	0.96	0.95	0.92
2^{-4}	0.97	0.97	0.97	0.95
2^{-6}	0.90	0.98	0.98	0.97
2^{-8}	0.93	0.92	0.92	0.92
2^{-10}	0.96	0.95	0.95	0.95
2^{-12}	0.98	0.97	0.97	0.97
2^{-14}	0.99	0.98	0.98	0.98
2^{-16}	0.99	0.99	0.99	0.99
2^{-18}	1.00	0.99	0.99	0.99
2^{-20}	1.00	0.99	0.99	0.99
p^N_{comp}	0.94	0.92	0.90	0.87

Table 5: Computed orders of convergence $p^N_{\varepsilon,comp}$, p^N_{comp} for $\frac{1}{V^*}(V_\varepsilon - \overline{V_B^{8192}})$ where V_ε is generated by (A^N_ε) for various values of ε, N and $\beta = 0.7$

$\varepsilon \backslash N$	32	64	128	256
2^{-0}	0.86	0.89	0.89	0.87
2^{-2}	0.91	0.92	0.90	0.84
2^{-4}	0.91	0.92	0.90	0.84
2^{-6}	0.78	0.91	0.91	0.88
2^{-8}	0.76	0.80	0.81	0.80
.	.	.	.	.
2^{-20}	0.76	0.80	0.81	0.80
p^N_{comp}	0.76	0.80	0.81	0.80

Table 6: Computed orders of convergence $p^N_{\varepsilon,comp}$, p^N_{comp} for $W_\varepsilon - \overline{W_B^{8192}}$ where W_ε is generated by (A^N_ε) for various values of ε, N and $\beta = 0.7$

The graphs in Figure 3 show where the error in the scaled velocity components is largest. For the x–direction and z–direction velocity components this is at points in the boundary layer on the surface of the wedge and for the y–direction component it is at points farthest from the surface of the wedge on the side of the domain closest to the leading edge.

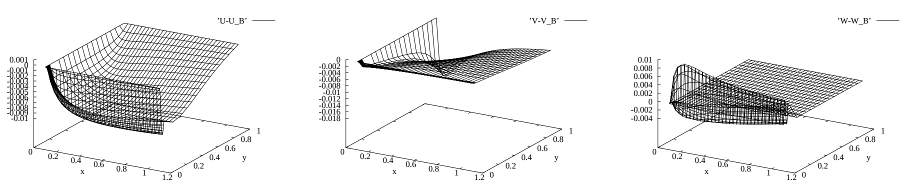

Figure 3: Graphs of $U_\varepsilon - \overline{U_B^{8192}}$, $\frac{1}{V^*}(V_\varepsilon - \overline{V_B^{8192}})$ and $W_\varepsilon - \overline{W_B^{8192}}$, for $\varepsilon = 2^{-8}$, N=32 and $\beta = 0.7$.

In Tables 7-11 we display the computed maximum pointwise errors of the approximations to the scaled first order derivatives of the velocity components. Since $D_yV = -D_xU$ it is only necessary to show the errors for one of these. We see that the behaviour is Re-uniform.

In Tables 12-16 we display the computed orders of convergence for the approximations of the first-order derivatives to the scaled velocity components $\sqrt{\varepsilon}D_y^-U_\varepsilon$, $D_y^-V_\varepsilon$, $\sqrt{\varepsilon}D_y^-W_\varepsilon$, $\frac{1}{V^*}D_x^-V_\varepsilon$ and $D_x^-W_\varepsilon$ obtained, respectively, from the corresponding Tables 7-11. We see that for each value of N the orders of convergence stabilize as $\varepsilon \to 0$ for $\beta = 0.7$. In additional computations, not reported here, similar behavior is observed for all $\beta \in [0, 1]$.

$\varepsilon \backslash N$	32	64	128	256	512
2^{-0}	9.07e-03	4.69e-03	2.50e-03	1.41e-03	8.60e-04
2^{-2}	1.78e-02	9.05e-03	4.67e-03	2.48e-03	1.39e-03
2^{-4}	3.34e-02	1.69e-02	8.59e-03	4.44e-03	2.37e-03
2^{-6}	5.84e-02	3.43e-02	1.73e-02	8.82e-03	4.56e-03
2^{-8}	5.82e-02	3.56e-02	2.11e-02	1.23e-02	7.08e-03
.	.	.	.	.	.
2^{-20}	5.83e-02	3.56e-02	2.11e-02	1.23e-02	7.08e-03

Table 7: Computed maximum pointwise error $E_\varepsilon^{\mathbf{N}}(\sqrt{\varepsilon}D_y^-U_\varepsilon)$ where U_ε is generated by (A_ε^N) for various values of ε, N and $\beta = 0.7$

$\varepsilon \backslash N$	32	64	128	256	512
2^{-0}	8.36e-02	4.78e-02	2.57e-02	1.32e-02	6.67e-03
2^{-2}	9.02e-02	5.10e-02	2.72e-02	1.41e-02	7.16e-03
2^{-4}	8.75e-02	4.87e-02	2.61e-02	1.35e-02	6.89e-03
2^{-6}	1.48e-01	8.75e-02	4.48e-02	2.32e-02	1.24e-02
2^{-8}	1.48e-01	9.08e-02	5.40e-02	3.16e-02	1.85e-02
.	.	.	.	.	.
2^{-20}	1.48e-01	9.08e-02	5.40e-02	3.16e-02	1.85e-02

Table 8: Computed maximum pointwise error $E_\varepsilon^{\mathbf{N}}(D_y^-V_\varepsilon)$ where V_ε is generated by (A_ε^N) for various values of ε, N and $\beta = 0.7$

$\varepsilon \backslash N$	32	64	128	256	512
2^{-0}	1.02e-02	5.24e-03	2.76e-03	1.55e-03	9.39e-04
2^{-2}	2.07e-02	1.05e-02	5.38e-03	2.82e-03	1.59e-03
2^{-4}	4.11e-02	2.07e-02	1.05e-02	5.38e-03	2.82e-03
2^{-6}	6.98e-02	4.11e-02	2.07e-02	1.05e-02	5.38e-03
2^{-8}	6.98e-02	4.27e-02	2.51e-02	1.44e-02	8.23e-03
.	.	.	.	.	.
2^{-20}	6.98e-02	4.27e-02	2.51e-02	1.44e-02	8.23e-03

Table 9: Computed maximum pointwise error $E_\varepsilon^{\mathbf{N}}(\sqrt{\varepsilon}D_y^-W_\varepsilon)$ where W_ε is generated by (A_ε^N) for various values of ε, N and $\beta = 0.7$

$\varepsilon \backslash N$	32	64	128	256	512
2^{-0}	9.10e-01	5.26e-01	3.07e-01	2.63e-01	3.35e-01
2^{-2}	4.81e-01	2.73e-01	1.82e-01	1.47e-01	9.22e-02
2^{-4}	4.22e-01	2.78e-01	2.01e-01	1.60e-01	1.22e-01
2^{-6}	3.83e-01	2.68e-01	2.09e-01	1.72e-01	1.39e-01
2^{-8}	3.49e-01	2.24e-01	1.69e-01	1.40e-01	1.21e-01
2^{-10}	3.33e-01	2.03e-01	1.38e-01	1.02e-01	7.77e-02
2^{-12}	3.26e-01	1.92e-01	1.23e-01	8.34e-02	5.68e-02
2^{-14}	3.22e-01	1.87e-01	1.15e-01	7.42e-02	4.65e-02
2^{-16}	3.20e-01	1.84e-01	1.12e-01	6.97e-02	4.14e-02
2^{-18}	3.20e-01	1.83e-01	1.10e-01	6.74e-02	3.89e-02
2^{-20}	3.19e-01	1.82e-01	1.09e-01	6.62e-02	3.76e-02

Table 10: Computed maximum pointwise error $E_\varepsilon^{\mathbf{N}}(D_x^- V_\varepsilon)$ where V_ε is generated by (A_ε^N) for various values of ε, N and $\beta = 0.7$

$\varepsilon \backslash N$	32	64	128	256	512
2^{-0}	5.35e-02	3.03e-02	1.63e-02	8.22e-03	4.19e-03
2^{-2}	3.03e-02	1.63e-02	8.34e-03	4.07e-03	1.91e-03
2^{-4}	3.56e-02	2.02e-02	1.06e-02	5.30e-03	2.50e-03
2^{-6}	3.60e-02	2.10e-02	1.14e-02	5.77e-03	2.76e-03
2^{-8}	3.60e-02	2.12e-02	1.17e-02	6.17e-03	3.09e-03
.	.	.	.	.	.
2^{-20}	3.60e-02	2.12e-02	1.17e-02	6.17e-03	3.09e-03

Table 11: Computed maximum pointwise error $E_\varepsilon^{\mathbf{N}}(D_x^- W_\varepsilon)$ in the subdomain $\overline{\Omega}_\varepsilon^N \bigcap [0.2, 1.1] \times [0, 1]$ where W_ε is generated by (A_ε^N) for various values of ε, N and $\beta = 0.7$

$\varepsilon \backslash N$	32	64	128	256
2^{-0}	0.95	0.91	0.83	0.71
2^{-2}	0.98	0.95	0.91	0.84
2^{-4}	0.98	0.97	0.95	0.91
2^{-6}	0.77	0.98	0.97	0.95
2^{-8}	0.71	0.75	0.78	0.80
.	.	.	.	.
2^{-20}	0.71	0.75	0.78	0.80
p_{comp}^N	0.71	0.75	0.78	0.80

Table 12: Computed orders of convergence $p_{\varepsilon,comp}^N$, p_{comp}^N for $\sqrt{\varepsilon}(D_y^- U_\varepsilon - D_y \overline{U_B^{8192}})$ where U_ε is generated by (A_ε^N) for various values of ε, N and $\beta = 0.7$

$\varepsilon \backslash N$	32	64	128	256
2^{-0}	0.81	0.90	0.95	0.99
2^{-2}	0.82	0.90	0.95	0.98
2^{-4}	0.84	0.90	0.95	0.97
2^{-6}	0.76	0.96	0.95	0.91
2^{-8}	0.71	0.75	0.77	0.78
.	.	.	.	.
2^{-20}	0.71	0.75	0.77	0.78
p^N_{comp}	0.71	0.75	0.77	0.78

Table 13: Computed orders of convergence $p^N_{\varepsilon,comp}$, p^N_{comp} for $(D^-_y V_\varepsilon - D_y \overline{V^{8192}_B})$ where V_ε is generated by (A^N_ε) for various values of ε, N and $\beta = 0.7$

$\varepsilon \backslash N$	32	64	128	256
2^{-0}	0.96	0.93	0.83	0.72
2^{-2}	0.98	0.96	0.93	0.83
2^{-4}	0.99	0.98	0.96	0.93
2^{-6}	0.76	0.99	0.98	0.96
2^{-8}	0.71	0.77	0.80	0.81
.	.	.	.	.
2^{-20}	0.71	0.77	0.80	0.81
p^N_{comp}	0.71	0.77	0.80	0.81

Table 14: Computed orders of convergence $p^N_{\varepsilon,comp}$, p^N_{comp} for $(D^-_y W_\varepsilon - D_y \overline{W^{8192}_B})$ where W_ε is generated by (A^N_ε) for various values of ε, N and $\beta = 0.7$

$\varepsilon \backslash N$	32	64	128	256
2^{-2}	0.82	0.58	0.31	0.67
2^{-4}	0.60	0.47	0.32	0.39
2^{-6}	0.51	0.36	0.28	0.31
2^{-8}	0.64	0.41	0.27	0.22
2^{-10}	0.72	0.55	0.44	0.39
2^{-12}	0.76	0.64	0.56	0.55
2^{-14}	0.79	0.70	0.64	0.67
2^{-16}	0.80	0.72	0.68	0.75
2^{-18}	0.80	0.74	0.71	0.79
2^{-20}	0.81	0.74	0.72	0.82
p^N_{comp}	0.79	0.41	0.28	0.31

Table 15: Computed orders of convergence $p^N_{\varepsilon,comp}$, p^N_{comp} for $\frac{1}{V^*}(D^-_x V_\varepsilon - D_x \overline{V^{8192}_B})$ where V_ε is generated by (A^N_ε) for various values of ε, N and $\beta = 0.7$

$\varepsilon \backslash N$	32	64	128	256
2^{-0}	0.82	0.90	0.98	0.97
2^{-2}	0.89	0.97	1.03	1.10
2^{-4}	0.82	0.92	1.01	1.09
2^{-6}	0.77	0.89	0.98	1.06
2^{-8}	0.76	0.86	0.93	1.00
.	.	.	.	.
2^{-20}	0.76	0.86	0.93	1.00
p^N_{comp}	0.82	0.90	0.98	0.97

Table 16: Computed orders of convergence $p^N_{\varepsilon,comp}$, p^N_{comp} for $(D^-_x W_\varepsilon - D_x \overline{W^{8192}_B})$ in the subdomain $\overline{\Omega}^N_\varepsilon \bigcap [0.2, 1.1] \times [0, 1]$ where W_ε is generated by (A^N_ε) for various values of ε, N and $\beta = 0.7$

5 Conclusion

We considered Prandtl's boundary layer equations for incompressible laminar flow past a three dimensional yawed wedge with angle $\beta\pi$, $\beta \in [0, 1]$. When the Reynolds number is large the solution of this problem has a parabolic boundary layer. We constructed a direct numerical method for computing approximations to the solution of this problem using a piecewise uniform fitted mesh technique appropriate to the parabolic boundary layer. We used the method to approximate the self–similar solution of Prandtl's problem in a finite rectangle excluding the leading edge of the wedge for various values of *Re* and β. We constructed and applied a special numerical method, related to the Blasius technique, to compute reference solutions to the problem. These were used to obtain approximate boundary conditions on the artificial boundaries of the computational domain and in the error analysis of the velocity components and their derivatives. Extensive numerical experiments indicated that the constructed direct numerical method is (Re, β)–uniform.

Acknowledgements

This research was supported by Enterprise Ireland grants SC-98-612 and SC/2000/070, Russian Foundation for Basic Research grant 01-01-01022 and National University of Singapore research projects R-151-000-024-112, R-151-000-025-112 and R-146-000-030-112.

References

[1] P. Farrell, A Hegarty, J.J.H. Miller, E. O'Riordan, G.I. Shishkin, *Robust Computational Techniques for Boundary Layers*, CRC Press, (2000).

[2] H. Schlichting, *Boundary Layer Theory*, 7^{th} edition, McGraw Hill, (1951).

[3] D.F. Rogers, *Laminar Flow Analysis*, Cambridge University Press, (1992).

[4] L. Rosenhead, *Laminar Boundary Layers*, Dover Publications, Inc. (1963)

[5] J. S. Butler, J.J.H. Miller, G.I. Shishkin, *A Reynolds–uniform method for Prandtl's boundary layer problem for flow past a wedge*, Inter. Journal for Numerical methods in Fluids; 43:903-913.